A Theoretical Comparison of Different Virtual Synchronous Generator Implementations on Inverters

Patrick Körner, Andrea Reindl, Hans Meier, Michael Niemetz
Faculty of Electrical Engineering and Information Technology
Ostbayerische Technische Hochschule Regensburg
Seybothstraße 2, 93053 Regensburg, Germany
Email: patrick1.koerner@st.oth-regensburg.de, andreareindl@ieee.org,
{hans.meier, michael.niemetz}@oth-regensburg.de

Keywords

≪Virtual Synchronous Generator (VSG)≫, ≪Virtual impedance≫, ≪Distributed Generation≫, ≪Voltage Source Inverter (VSI)≫, ≪Grid-connected inverter≫

Abstract

The goal to overcome the global climate crisis leads to a rising demand for the usage of Renewable Energy Sources (RES). Decentralized control strategies are needed to allow the integration of RES into the grid. The Virtual Synchronous Generator (VSG) is proposed as a method to add virtual inertia to the grid by emulating the rotating mass of a Synchronous Generator (SG) on the control algorithm of an inverter. This paper presents the VSG control structure as well as the mathematical description in a unified form. Due to the fact that classical droop control can be seen as a special form of the VSG, their correlation is highlighted by evaluating the steady state output characteristics of the inverter. Furthermore, a theoretical comparison between different VSG topologies, including the VISMA-Method 2 and the synchronverter, is given. In order to achieve better voltage stability, principles to add virtual impedance to the inverter's output are described.

Introduction

The rising penetration of renewable energy sources in the grid leads to the need for decentralized and communication-less control strategies. Furthermore, microgrids consisting of many Distributed Generators (DGs) are emerging. Power electronic devices, called inverters, are connecting these DGs to the grid. Inverters are usually supplied from a DC-line or a DC-stage [1]. The two categories, Current Source Inverter (CSI) and Voltage Source Inverter (VSI), can be classified into grid-forming, grid-feeding and grid-supporting converters. CSIs hardly have the ability to regulate the grid voltage. Due to this, it can't operate in islanded mode without having a grid-forming VSI in parallel. [2]

Large synchronous generators in centralized power plants can operate as grid-forming voltage sources that have good load sharing characteristics and provide large inertia to the grid [3, 4]. On the other hand, the increasing number of inverters that do not have rotating masses and therefore stored kinetic energy, decreases the overall inertia, which results in a decreasing reliability and supply quality of the grid [5–8].

Droop control is an established method to allow a parallel operation of DGs. This control technique emulates the steady-state droop characteristics of the governor and the Automatic Voltage Regulator (AVR) of a SG, allowing participation in frequency and voltage regulation [4]. This primary control method has a lack of inertia [7, 8]. As for, this results in a higher Rate of Change of Frequency (RoCoF) during transient load peaks or grid faults, than with a SG.

The VSG is a proposed solution for this problem. By implementing the droop characteristics (P-ω-droop and Q-V-droop) and the small-signal model of a SG on the control algorithm of an inverter, virtual inertia

can be added to the grid. The key is the emulation of the swing equation of a SG and a suitable Energy Storage System (ESS).

It has to be taken into account that there are current-controlled and voltage-controlled VSGs. The Virtual Synchronous Machine VISMA-Method 1 [9] is a current-controlled VSG, while the VISMA-Method 2 [10], synchronverters [11–13] and VSGs only based on the electromechanical swing equation [14–19] are voltage-controlled ones. Since the CSI's control strategies rely on a Phase-Locked Loop (PLL) to obtain the angular frequency from the grid, it can not operate in islanded mode [20]. Current research mostly focuses on enhanced control strategies for VSG implementations on VSIs, to achieve better transient characteristics [16]. In the reference [17] a new damping strategy for active power oscillation damping was developed and verified by experimental measurements.

This paper focuses on VSGs for VSIs in order to allow an islanded operation and to draw a comparison to classical droop control [21]. Therefore a brief description of the control algorithm is given in the next Section by using a unified control structure. The following Section presents a method used in high order models, to add virtual impedance to the system, while the last Section closes with a comparison between the VISMA-Method 2 and the synchronverter.

Unified structure of a Virtual Synchronous Generator

The basic control structure of a VSG, consisting of a virtual inertia emulating block and a virtual AVR, is shown in Fig. 1. The three-phase output of the inverter is filtered through a LC-filter (L_f,C_f). A cur-

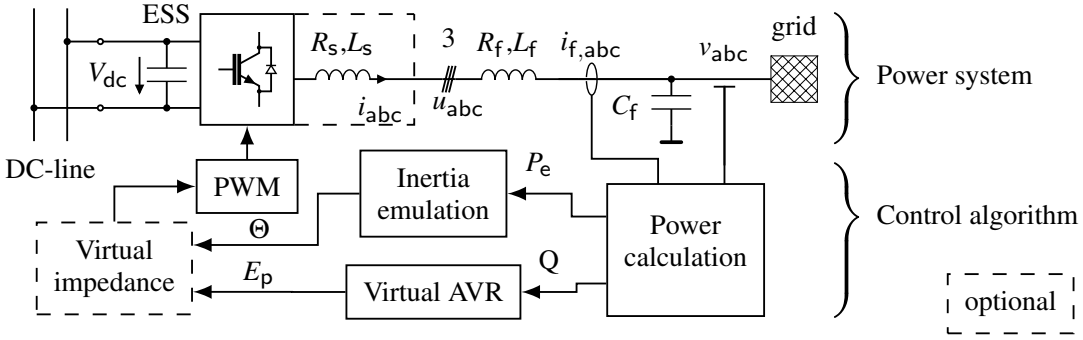

Fig. 1: Basic control structure of the VSG algorithm on a VSI for inertia emulation in a distributed generation system that is connected to the grid [22,23] and adds virtual impedance (R_s,L_s) to the output. Combining the control algorithm with an suitable ESS adds virtual inertia to the grid by emulating the mechanical swing equation of a SG in the inertia emulating block.

rent and voltage measurement is used to obtain the corresponding output characteristics. The literature describes various approaches for applying the control structure in different frame representations. Either the control is based on the natural *abc*-frame [24], the stationary αβ-frame [25] or the synchronous rotating *dq*-frame [1,17,19,26,27]. This implies the usage of Clarke- and/or Park-transformation. Reference [28] describes a method called "double decoupled synchronous reference frame", which can be used to control a single-phase or an unbalanced three-phase VSG by using a combination of all three frames [23].

Active power control

The active power control on a VSG is done by emulating a virtual governor and the mechanical swing equation, the latter is the key to add virtual inertia to the system. The obtained active power P_e is fed into the VSG model. As an output, the angular position $\Theta = \int \omega dt$ of the rotor field to the reference axis is calculated. Whereas ω is the angular frequency. [9]

The swing equation

$$J \cdot \ddot{\Theta} = T_m - T_e - D_m \cdot \dot{\Theta} \tag{1}$$

describes the mechanical behavior of the rotor [29]. Where $\ddot{\Theta}$ is the angular acceleration, J is the moment of inertia, T_m is the mechanical torque of the prime mover, T_e is the electrical torque and D_m is the damping coefficient due to mechanical friction [21]. All VSG implementations (except VISMA) use a modified version of (1) since it is more accurate to model the damping effect with the term $D_\mathrm{p} \cdot (\dot{\Theta} - \dot{\Theta}_0)$, which represents the much larger electrical damping effects [21]. This damping is caused by induction currents in the amortisseur windings due to a relative motion ($\Delta\dot{\Theta} = \dot{\Theta} - \dot{\Theta}_0$) between the rotor and the stator magnetic field [21]. As follows, the swing equation should be rewritten as:

$$J \cdot \ddot{\Theta} = T_\mathrm{m} - T_\mathrm{e} - D_\mathrm{p} \cdot (\dot{\Theta} - \dot{\Theta}_0) \tag{2}$$

Since the relative difference between $\dot{\Theta}$ and $\dot{\Theta}_0$ is negligible, (2) can be multiplied with the nominal angular frequency $\dot{\Theta}_0 = \omega_0$ on both sides [15, 21], which leads to:

$$J \cdot \omega_0 \cdot \frac{\mathrm{d}\omega}{\mathrm{d}t} = P_\mathrm{m} - P_\mathrm{e} - D \cdot (\omega - \omega_0) \tag{3}$$

where P_m and P_e are the mechanical and electrical powers and $J \cdot \omega_0$ is called the inertia constant of the synchronous generator.

The virtual governor acts like a deviating secondary frequency regulator and can be written as [1]:

$$P_\mathrm{m} = P_0 - k_\omega \cdot (\omega - \omega_0) \tag{4}$$

P_0 is the nominal active power and k_ω represents the governor droop factor. This factor usually is a proportional controller or a PI controller and can be realized to only act, when the deviation $(\omega - \omega_0)$ exceeds certain values [21]. The mechanical governor of a SG usually has a large delay, therefore an exact mechanical analogon would include a first order lag unit with parameter T_d [8].

When using the Laplace transformation on (3) and (4), the result can be combined and simplified to

$$P_0 - P_\mathrm{e} - k_\mathrm{p} \cdot (\omega - \omega_0) = J \cdot \omega_0 \cdot s \cdot \omega \tag{5}$$

where $k_\mathrm{p} = D_\mathrm{p} + k_\omega$ is used as droop factor. Furthermore the equation for the angular frequency can be rewritten as:

$$\omega = \frac{1}{J \cdot \omega_0 \cdot s + k_\mathrm{p}} \cdot (P_0 - P_\mathrm{e} + k_\mathrm{p} \cdot \omega_0) \tag{6}$$

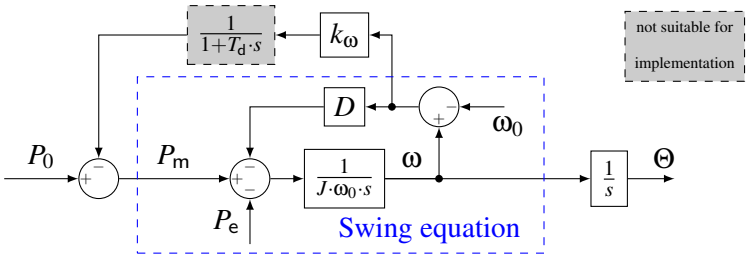

Fig. 2: Unification of the active power control block for the VSG, consisting of the swing equation with a damping term D, the governor [21] and the modeling of the mechanical governor delay T_d [8]. The governor is realized as a proportional droop controller with droop factor k_ω. As an output, the angular position Θ is obtained.

The analysis of the system's state space eigenvalues in the references [7, 8] proves, that the in Fig. 2 shown model with and without the optional governor delay is stable. It can be observed, that increasing values for the inertia constant $J \cdot \omega_0$ leads to a convergence of the eigenvalues onto the origin. Thus, $J \cdot \omega_0$ affects the oscillation frequency of the active power during transient events while its damping effect can be neglected. As for an increasing T_d, the eigenvalue analysis and the simulations results from [7] show,

that the system gets more oscillatory and has higher RoCoF. Therefore, the mechanical governor delay should not be emulated in the VSG. [7, 8]

Virtual inertia can only be emulated, when the ESS (cf. Fig. 1) is able to supply the VSI with the needed electrical energy [3, 8].

Reactive power control

The virtual automatic voltage regulator is realized in the reactive power control (Fig. 3), same as with a SG [25]. An internal voltage reference V_{ref} is controlled by drooping the reactive power deviation between the measured reactive power Q and the setpoint Q_0 with the factor D_{q} [14]. Where V_0 is the voltage setpoint. The low pass filter represents the exciter system whereas for Q-V-droop, T_{f} should be set as the time constant of the LC power filter (Fig. 1) in order to achieve better reactive power sharing among all VSIs [26]. E_{p} is the amplitude of the back Electromotive Force (EMF), which is used to calculate the output voltage u_{abc} of the VSI [25].

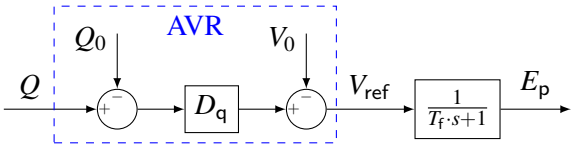

Fig. 3: Reactive power control by implementing the AVR as a proportional Q-V-droop controller with an additional low pass filter as representation for the exciter system [26]. The output E_{p} is the amplitude of the back EMF.

The AVR can be realized differently on each VSG and therefore it is not possible to present a unified control structure. For further interest, reference [26] investigates different AVRs for VSGs.

Steady state output characteristics

The VSI can take an active role in frequency- and voltage-control, by applying the mentioned drooping techniques. These steady state output characteristics (Fig. 4) allow parallelization of multiple VSGs.

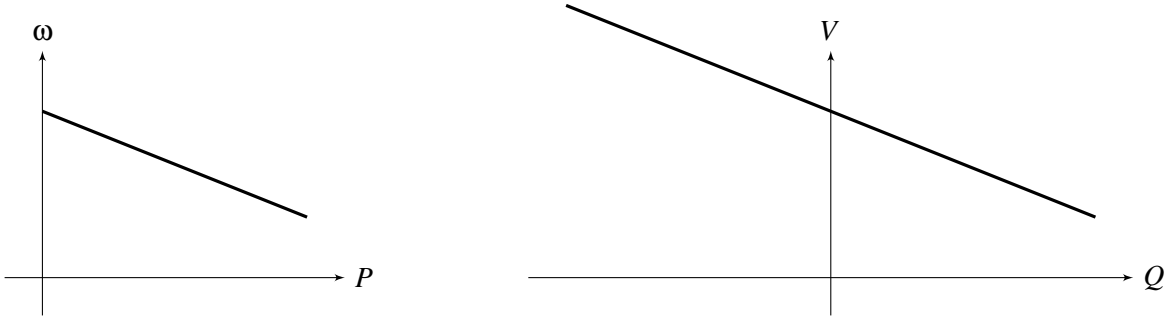

(a) P-ω-droop (b) Q-V-droop

Fig. 4: Steady state output characteristics of a VSG for active and reactive power [30].

To draw a comparison to classical droop control, the virtual moment of inertia J in (6) can be removed by setting it to 0, which leads to the equation for classical droop control [8]:

$$\omega = \frac{1}{k_{\mathsf{p}}} \cdot (P_0 - P_{\mathsf{e}}) + \omega_0 \tag{7}$$

Due to the missing first order lag unit, which inserts a frequency drooping delay, (7) has worse transient characteristics than (6). This results in smaller values for the RoCoF. As a consequence, existing virtual inertia improves the transient abilities and enhances the frequency support of the inverter [4] as experimental results [8] and simulations [31] show.

Virtual Winding for High Order VSG models

Virtual impedance ($R_\mathsf{s}, L_\mathsf{s}$ in Fig. 1) is added, because the stator impedance of a SG typically is in the range of $1.5\,\text{p.u.} - 2.0\,\text{p.u.}$, while the output filter impedance of a VSI is significantly lower ($0.05\,\text{p.u.} - 0.2\,\text{p.u.}$) [13, 32, 33]. Furthermore, the LC-filter values are fixed due to the switching frequency of the VSI and it is more energy efficient to rely on changeable virtual resistances, rather than fixed, non-virtual ones [21]. A larger output impedance leads to more robustness against voltage fluctuations [13] and enhances the voltage profile [34]. There are different approaches to add virtual impedance to the output of a VSI. One is referred as virtual winding of the stator and is only used in high order VSG models, that try to mimic the geometry of the stator inductances [26]. For the interested reader, a brief mathematical description of the SG geometry is given in [11, 35].

Assuming a constant excitation current i_f for the rotor field and $\dot{\Theta} \approx \text{const.}$, the induced EMF $e = \begin{bmatrix} e_\mathsf{a} & e_\mathsf{b} & e_\mathsf{c} \end{bmatrix}^T$ can be written as an expression of the mutual inductance M_f between the stator and rotor windings:

$$e = \dot{\Theta} \cdot M_\mathsf{f} \cdot i_\mathsf{f} \cdot \widetilde{\sin}(\Theta) \approx E_\mathsf{p} \cdot \widetilde{\sin}(\Theta) \tag{8}$$

$$\widetilde{\sin}(\Theta) = \begin{bmatrix} \sin(\Theta) & \sin\left(\Theta - \frac{2\pi}{3}\right) & \sin\left(\Theta + \frac{2\pi}{3}\right) \end{bmatrix}^T \tag{9}$$

The expression $\widetilde{\sin}(\Theta)$ is given due to the geometry of the stator windings. [11] Following, the output voltage vector $u_\mathsf{abc} = \begin{bmatrix} u_\mathsf{a} & u_\mathsf{b} & u_\mathsf{c} \end{bmatrix}^T$ can be defined via a voltage drop due to the output current $i_\mathsf{abc} = \begin{bmatrix} i_\mathsf{a} & i_\mathsf{b} & i_\mathsf{c} \end{bmatrix}^T$:

$$u_\mathsf{abc} = e - R_\mathsf{s} \cdot i_\mathsf{abc} - L_\mathsf{s} \cdot \frac{\mathrm{d}i_\mathsf{abc}}{\mathrm{d}t} \tag{10}$$

When implementing (8) and (10) in the control algorithm, a virtual impedance can be added to the VSI's output.

Experimental results, that prove the concept of virtual impedance implementation, can be obtained from [13]. Reference [32] compares an inverter, where virtual impedance is implemented, to one, where none is added. The overall benefits are verified via simulation and measurements [32, 36].

Different Virtual Synchronous Generator Implementations

In this Section, a discussion of different VSG topologies, including the VISMA-Method 2 and the synchronverter, is given. VSG implementations only based on the mechanical swing equation are not shown. Therefore the authors refer to the comprehensive review in reference [20] and states that the control structure in Fig. 2 is a unified one.

VISMA

The voltage to current model VISMA-Method 1 was invented by Beck and Hesse in 2007 and is the most accurate and highest order model of a SG [37]. Their improved version called VISMA-Method 2 is a current to voltage model which is more suitable for implementation, due to the more common Pulse-Width Modulation (PWM) inverters. Since it is considered as a 7^{th} order model, there are only a few simplifications that are made in comparison to a real SG. These include the neglection of the winding coupling, which would result in additional mutual inductances, as well as the effect of damping in the windings. [20]

Fig. 5 shows the implementation of VISMA-Method 2, which includes the virtual winding, the virtual governor and the swing equation. The corresponding literature does not state what exact expression is used for $f(s)$ in the damping term of the swing equation [21]. Furthermore, Fig. 5 does not include the virtual AVR, which is used to calculate E_p for the back EMF (Fig. 3).

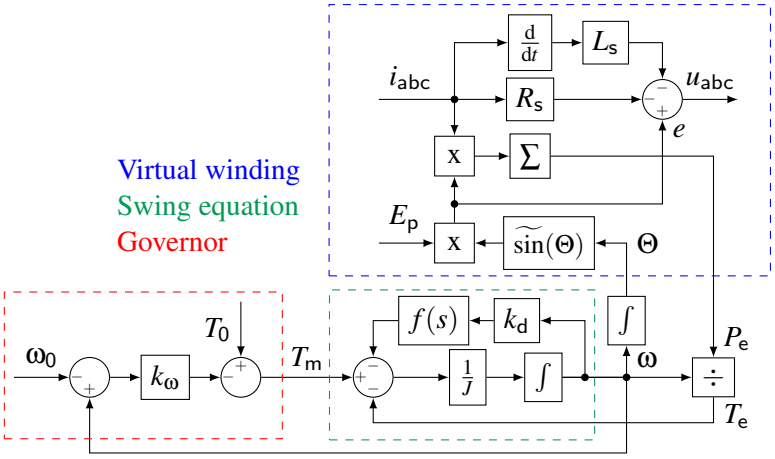

Fig. 5: Control structure of the VISMA-Method 2 [10], which includes the modeling of the virtual winding and the mechanical swing equation in form of torque, as well as the virtual governor.

The VISMA-Method 2 can operate without further hardware configurations as a grid supporting inverter in grid-connected and islanded mode. However, it has a poor dynamic response time when changing from grid-connected to islanded mode. When a change in grid frequency happens (in a poor grid for example), it shows a large RoCoF response. Advantages of the VISMA are a small frequency deviation and a small RoCoF response during load disturbances. The same applies to the dynamic response during power steps. [20]

Due to VISMA's complexity, a lot of computation power is required to run the algorithm on a VSI. Therefore, the VISMA is hardly used in real power systems. [20]

Synchronverter

The synchronverter is a 2nd order model of the SG and was firstly introduced in 2009 [20, 29]. Both authors presented further enhancements, that increases the virtual impedance and that allows the synchronverter to self-synchronize itself before connecting to the grid [11, 13, 38].

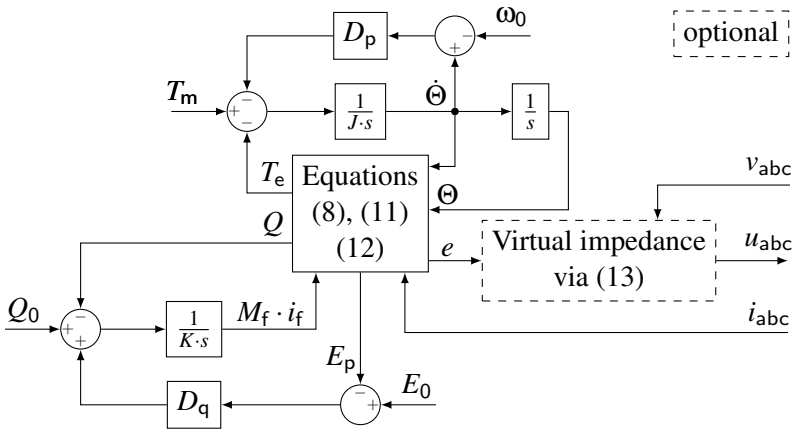

Fig. 6: Control structure of the synchronverter [29], based on the electromagnetic equations, which includes an optional virtual impedance emulating block [36].

Same as the VISMA, the synchronverter realizes the swing equation and therefore the active power control in form of torque. A simplification is made by not emulating the virtual winding and therefore the VSI only has an output impedance that is determined by the output filter (R_f, L_f, C_f in Fig. 1). [20] Synchronverter's control structure is shown in Fig. 6, whereas the equations used in the model are the

following [11, 13]:

$$T_\mathsf{e} = M_\mathsf{f} \cdot i_\mathsf{f} \cdot \langle i_\mathsf{abc}, \widetilde{\sin}(\Theta) \rangle \tag{11}$$

$$Q = \dot{\Theta} \cdot M_\mathsf{f} \cdot i_\mathsf{f} \cdot \langle i_\mathsf{abc}, \widetilde{\sin}(\Theta - \frac{\pi}{2}) \rangle \tag{12}$$

$$u_\mathsf{abc} = \frac{(n-1) \cdot v_\mathsf{abc} + e}{n} \tag{13}$$

$$\Leftrightarrow e = v_\mathsf{abc} + n \cdot (u_\mathsf{abc} - v_\mathsf{abc}) = v_\mathsf{abc} + n \cdot \Delta u \tag{14}$$

Although the virtual winding technique is missing, reference [13] stated a simple method to virtually increase the output impedance of the LC-filter with the factor n by implementing (13) in the algorithm. This imposes u_abc as the output voltage of the inverter, although v_abc (cf. Fig. 1) is used in the calculation. It follows that $R_\mathsf{s} = (n-1) \cdot R_\mathsf{f}$ and $L_\mathsf{s} = (n-1) \cdot L_\mathsf{f}$. The resulting one phase model of the synchronverter (Fig. 7) can be obtained from (14). Using this method results in a more robust design and positively influences the current peak values during asymmetric faults [13, 39, 40].

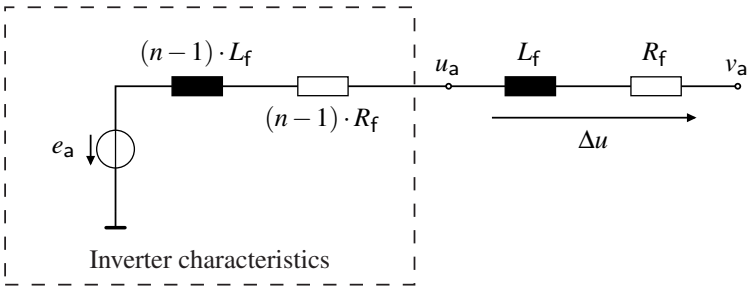

Fig. 7: One phase model of a synchronverter that adds virtual impedance (the ones multiplied by $(n-1)$) to the inverter's output. As a result, the overall output impedance of the inverter is multiplied by the factor n. [13]

Further enhancements for an active power oscillation suppression can be added to the swing equation of the synchronverter in form of an additional virtual damping term [36].

In comparison to the VISMA-Method 2, the implementation of the synchronverter is far simpler to realize and it has better dynamic characteristics when changes from grid-connected to islanded mode occur. On the other hand, it shows a larger frequency deviation response when changes in the grid frequency happen and it has worse dynamic properties during power steps or load disturbances than the VISMA. [20]

Synchronverter is a suitable solution for HVDC-transmission, where it can work as a synchronous motor at the sending-end and as a SG at the receiving-end [12].

Conclusion

This paper stated the importance of VSGs for future renewable energy sources dominated grid compositions, including HVDC-transmission and microgrids. Their ability to decrease the RoCoF and damp power oscillations was shown by the mathematical investigation of a unified VSG control structure. The emulation of the swing equation in compound with a ESS adds virtual inertia to the grid. The steady state output characteristics of a VSG were shown in order to draw a comparison to classical droop control. The VISMA-Method 2 and the synchronverter implementations were presented while stating the difference between both of them. For both models, a comparison of their behavior during load and frequency changes and changes from grid-connected to islanded mode was given. Since the synchronverter is one of the most promising solutions and can be implemented with reasonable computation effort, further enhancements were listed and referenced. As one of the most important design enhancements, the method

to implement virtual impedance was shown for both the VISMA-Method 2 and the synchronverter. The verification of the obtained theoretical statements was done by referencing corresponding simulation results and experimental measurements from the literature. An investigation of other VSG topologies only based on the swing equation is left for future work.

References

[1] X. Meng, J. Liu, and Z. Liu, "A Generalized Droop Control for Grid-Supporting Inverter Based on Comparison Between Traditional Droop Control and Virtual Synchronous Generator Control," *IEEE Trans. on Power Electronics*, pp. 5416–5438, 2019.

[2] J. Rocabert, A. Luna, F. Blaabjerg, and P. Rodríguez, "Control of Power Converters in AC Microgrids," *IEEE Trans. on Power Electronics*, pp. 4734–4749, 2012.

[3] P. Unruh, M. Nuschke, P. Strauß, and F. Welck, "Overview on Grid-Forming Inverter Control Methods," *Energies*, p. 2589, 2020.

[4] M. Chen, D. Zhou, and F. Blaabjerg, "Impact of Synchronous Generator Replacement with VSG on Power System Stability," in *IEEE 21st Workshop on Control and Modeling for Power Electronics*, 2020, pp. 1–7.

[5] J. Driesen and K. Visscher, "Virtual Synchronous Generators," in *IEEE Power and Energy Society General Meeting - Conversion and Delivery of Electrical Energy in the 21st Century*, 2008, pp. 1–3.

[6] M. H. J. Bollen, Y. Yang, and F. Hassan, "Integration of Distributed Generation in the Power System - A Power Quality Approach," in *13th International Conference on Harmonics and Quality of Power*, 2008, pp. 1–8.

[7] J. Liu, Y. Miura, and T. Ise, "Dynamic Characteristics and Stability Comparisons between Virtual Synchronous Generator and Droop Control in Inverter-Based Distributed Generators," in *International Power Electronics Conference (IPEC-Hiroshima 2014 - ECCE ASIA)*, 2014, pp. 1536–1543.

[8] J. Liu, Y. Miura, and T. Ise, "Comparison of Dynamic Characteristics Between Virtual Synchronous Generator and Droop Control in Inverter-Based Distributed Generators," *IEEE Trans. on Power Electronics*, pp. 3600–3611, 2016.

[9] Y. Chen, R. Hesse, D. Turschner, and H.-P. Beck, "Improving the Grid Power Quality Using Virtual Synchronous Machines," in *International Conference on Power Engineering, Energy and Electrical Drives*, 2011, pp. 1–6.

[10] Y. Chen, R. Hesse, D. Turschner, and H.-P. Beck, "Comparison of methods for implementing virtual synchronous machine on inverters," *Renewable Energy and Power Quality Journal*, pp. 734–739, 2012.

[11] Q.-C. Zhong and G. Weiss, "Synchronverters: Inverters That Mimic Synchronous Generators," *IEEE Trans. on Industrial Electronics*, pp. 1259–1267, 2011.

[12] R. Aouini, B. Marinescu, K. Ben Kilani, and M. Elleuch, "Synchronverter-Based Emulation and Control of HVDC Transmission," *IEEE Trans. on Power Systems*, pp. 278–286, 2016.

[13] V. Natarajan and G. Weiss, "Synchronverters With Better Stability Due to Virtual Inductors, Virtual Capacitors, and Anti-Windup," *IEEE Trans. on Industrial Electronics*, pp. 5994–6004, 2017.

[14] Y. Du, J. M. Guerrero, L. Chang, J. Su, and M. Mao, "Modeling, Analysis, and Design of a Frequency-Droop-Based Virtual Synchronous Generator for Microgrid Applications," in *IEEE ECCE Asia Downunder*, 2013, pp. 643–649.

[15] M. Guan, W. Pan, J. Zhang, Q. Hao, J. Cheng, and X. Zheng, "Synchronous Generator Emulation Control Strategy for Voltage Source Converter (VSC) Stations," *IEEE Trans. on Power Systems*, pp. 3093–3101, 2015.

[16] J. Liu, Y. Miura, H. Bevrani, and T. Ise, "Enhanced Virtual Synchronous Generator Control for Parallel Inverters in Microgrids," *IEEE Trans. on Smart Grid*, pp. 2268–2277, 2017.

[17] M. Chen, D. Zhou, and F. Blaabjerg, "Active Power Oscillation Damping Based on Acceleration Control in Paralleled Virtual Synchronous Generators System," *IEEE Trans. on Power Electronics*, pp. 9501–9510, 2021.

[18] X. Xiong, C. Wu, and F. Blaabjerg, "An Improved Synchronization Stability Method of Virtual Synchronous Generators Based on Frequency Feedforward on Reactive Power Control Loop," *IEEE Trans. on Power Electronics*, pp. 9136–9148, 2021.

[19] X. Xiong, C. Wu, P. Cheng, and F. Blaabjerg, "An Optimal Damping Design of Virtual Synchronous Generators for Transient Stability Enhancement," *IEEE Trans. on Power Electronics*, pp. 11 026–11 030, 2021.

[20] M. Chen, D. Zhou, and F. Blaabjerg, "Modelling, Implementation, and Assessment of Virtual Synchronous Generator in Power Systems," *Journal of Modern Power Systems and Clean Energy*, pp. 399–411, 2020.

[21] X. Meng, Z. Liu, J. Liu, T. Wu, S. Wang, and B. Liu, "Comparison between Virtual Synchronous Generator and Droop Controlled Inverter," in *IEEE 2nd Annual Southern Power Electronics Conference (SPEC)*. Piscataway, NJ: IEEE, 2016, pp. 1–6.

[22] T. Shintai, Y. Miura, and T. Ise, "Oscillation Damping of a Distributed Generator Using a Virtual Synchronous Generator," *IEEE Trans. on Power Delivery*, pp. 668–676, 2014.

[23] J. Liu, M. Yushi, T. Ise, J. Yoshizawa, and K. Watanabe, "Parallel Operation of a Synchronous Generator and a Virtual Synchronous Generator under Unbalanced Loading Condition in Microgrids," in *IEEE 8th International Power Electronics and Motion Control Conference (IPEMC-ECCE Asia)*, 2016, pp. 3741–3748.

[24] L. Xia and L. Hai, "Comparison of Dynamic Power Sharing Characteristics between Virtual Synchronous Generator and Droop Control in Inverter-Based Microgrid," in *IEEE 3rd International Future Energy Electronics Conference and ECCE Asia (IFEEC 2017 - ECCE Asia)*. IEEE, 2017, pp. 1548–1552.

[25] O. Mo, S. D'Arco, and J. A. Suul, "Evaluation of Virtual Synchronous Machines With Dynamic or Quasi-Stationary Machine Models," *IEEE Trans. on Industrial Electronics*, pp. 5952–5962, 2017.

[26] M. Chen, D. Zhou, and F. Blaabjerg, "Voltage Control Impact on Performance of Virtual Synchronous Generator," in *International Power Electronics Conference (IPEC-Hiroshima - ECCE ASIA)*, 2014, pp. 1981–1986.

[27] C. Zhang, Q. Zhong, J. Meng, X. Chen, Q. Huang, S. Chen, and Z. Lv, "An Improved Synchronverter Model and its Dynamic Behaviour Comparison with Synchronous Generator," in *2nd IET Renewable Power Generation Conference (RPG 2013)*, 2013, pp. 1–4.

[28] Y. Hirase, O. Noro, E. Yoshimura, H. Nakagawa, K. Sakimoto, and Y. Shindo, "Virtual Synchronous Generator Control with Double Decoupled Synchronous Reference Frame for Single-Phase Inverter," in *International Power Electronics Conference (IPEC-Hiroshima 2014 - ECCE ASIA)*, 2014, pp. 1552–1559.

[29] Q. Zhong and G. Weiss, "Static Synchronous Generators for Distributed Generation and Renewable Energy," in *IEEE/PES Power Systems Conference and Exposition*, 2009, pp. 1–6.

[30] J. Roldan-Perez, A. Rodriguez-Cabero, and M. Prodanovic, "Harmonic Virtual Impedance Design for Parallel-Connected Grid-Tied Synchronverters," *IEEE Journal of Emerging and Selected Topics in Power Electronics*, pp. 493–503, 2019.

[31] G. Júnior, T. Nascimento, and L. S. Barros, "Comparison of Virtual Synchronous Generator Strategies for Control of Distributed Energy Sources and Power System Stability Improvement," *Simpósio Brasileiro de Sistemas Elétricos - SBSE*, 2020.

[32] R. Rosso, S. Engelken, and M. Liserre, "Robust Stability Analysis of Synchronverters Operating in Parallel," *IEEE Trans. on Power Electronics*, pp. 11 309–11 319, 2019.

[33] L. Zhang, L. Harnefors, and H.-P. Nee, "Power-Synchronization Control of Grid-Connected Voltage-Source Converters," *IEEE Trans. on Power Systems*, pp. 809–820, 2010.

[34] A. Tarrasó, J. I. Candela, J. Rocabert, and P. Rodriguez, "Grid Voltage Harmonic Damping Method for SPC based Power Converters with Multiple Virtual Admittance Control," in *IEEE Energy Conversion Congress and Exposition (ECCE)*, 2017, pp. 64–68.

[35] E. Brown and G. Weiss, "A study of the use of synchronverters for grid stabilization using simulations in SimPower," Master's thesis, Tel Aviv University, 2015.

[36] Z. Shuai, W. Huang, Z. J. Shen, A. Luo, and Z. Tian, "Active Power Oscillation and Suppression Techniques Between Two Parallel Synchronverters During Load Fluctuations," *IEEE Trans. on Power Electronics*, pp. 4127–4142, 2020.

[37] H.-P. Beck and R. Hesse, "Virtual Synchronous Machine," in *9th International Conference on Electrical Power Quality and Utilisation*, 2007, pp. 1–6.

[38] Q.-C. Zhong, P.-L. Nguyen, Z. Ma, and W. Sheng, "Self-Synchronized Synchronverters: Inverters Without a Dedicated Synchronization Unit," *IEEE Trans. on Power Electronics*, pp. 617–630, 2014.

[39] R. Rosso, J. Cassoli, G. Buticchi, S. Engelken, and M. Liserre, "Robust Stability Analysis of LCL Filter Based Synchronverter Under Different Grid Conditions," *IEEE Trans. on Power Electronics*, pp. 5842–5853, 2019.

[40] L. He, Z. Shuai, X. Zhang, X. Liu, Z. Li, and Z. J. Shen, "Transient Characteristics of Synchronverters Subjected to Asymmetric Faults," *IEEE Trans. on Power Delivery*, pp. 1171–1183, 2019.